

## THE INFLUENCE OF DISDROMETER CHANNELS ON SPECIFIC ATTENUATION DUE TO RAIN OVER MICROWAVE LINKS IN SOUTHERN AFRICA

O. Adetan\* and T. Afullo\*\*

\* *Discipline of Electrical, Electronic and Computer Engineering School of Engineering, University of KwaZulu-Natal, Private Bag X54001, Durban 4041, South Africa E-mail: [211559250@stu.ukzn.ac.za](mailto:211559250@stu.ukzn.ac.za), or [oadetan@gmail.com](mailto:oadetan@gmail.com)*

\*\* *Discipline of Electrical, Electronic and Computer Engineering, School of Engineering, University of KwaZulu-Natal, Private Bag X54001, Durban 4041, South Africa E-mail: [afullot@ukzn.ac.za](mailto:afullot@ukzn.ac.za)*

**Abstract:** The influence of raindrop channels on the measured rain rate and specific rainfall attenuation in Durban (29°52'S, 30° 58'E), South Africa for six rain rate values: 1.71, 4.46, 22.97, 64.66, 77.70 and 84.76 mm/hr selected from the rain events that occurred on the 27th December 2008 is analyzed in this work. Consecutive and alternate drop channels are removed to study the influence of raindrop diameters on the overall measured rain rate. The three-parameter gamma and lognormal models are used for the purpose of analysis. In general and for the two models considered, the lower channels (channels 1 to 5) do not alter significantly the overall rain rate and equally produce minimal attenuation. The critical raindrop channels contributing the larger percentage to the overall rain rate are created by  $D \geq 0.771\text{mm}$ . The deviations of the measured and estimated rain rates are very small for all the rainfall rates selected. The estimation of the specific rain attenuation at frequency of 19.5 GHz is also discussed. The error estimation using the two models are also analysed.

**Keywords:** Raindrop size distribution, raindrop channels, specific rainfall attenuation, root mean square error.

### 1. INTRODUCTION

The failure and inability of service providers to constantly meet the design target of 99.99 % availability of the line-of-sight (LOS) microwave links has caused several rifts between the operators and the consumers. The non-availability of the links is predominantly due to propagation impairments along the link. These propagation effects include cloud, fog, gas attenuation, rain and atmospheric scintillation. Of these impairments, rain attenuation is the dominant and most disturbing atmospheric impairment for satellite communications systems operating at any frequency above 10 GHz. Rain attenuation may be due to rain at any point along the propagation path [1-4]. According to *Safaai-Jazi et al.* [5], attenuation below 6 dB is caused mainly by stratiform rain, while attenuation more than 6 dB may largely be attributed to thunderstorms in the frequency range of 12-30 GHz. A good knowledge of the raindrop size distribution (DSD) is essential in the estimation of the rain attenuation at the radio frequency band because it governs all the microwave and rainfall integral relations. It is a known fact that modeling of DSD varies from one region to another. Drop size

distribution modeling in temperate region; characterized by moderate rainfall is well suited with models such as proposed by *Marshall and Palmer* [6], *Laws and Parsons* [7] and similar negative exponential models [8]. The globally accepted *Ajayi and Olsen* [9] and the *Ajayi and Adimula* [10] lognormal distribution models better describe the drops size distributions modeling in the tropical regions, characterized by heavy rainfall.

In this work, we analyze the specific contribution of individual raindrop channels to the overall measured rainfall rate and specific rain attenuation in southern Africa. The estimation of the specific rainfall attenuation at 19.5 GHz is also discussed. Six (6) rain rate values are selected from the rain events that took place in Durban (29°52'S, 30° 58'E) on the 27<sup>th</sup> of December 2008 using the Joss-Waldvogel RD-80 disdrometer measurement. The rain rates are 1.71, 4.46, 22.97, 64.66, 77.70 and 84.76 mm/hr representing stratiform and convective rainfall types as defined by [1]. The three-parameter gamma and lognormal DSD models are used for the purpose of analysis. The paper is divided into five sections. Related works done in South Africa and other regions is discussed in section 2. Data analysis, DSD models and specific attenuation

are covered in section 3. The results and discussion on the influence (contributions) of individual channels to overall measured rain rate and the estimation of the specific attenuation at 19.5 GHz are discussed in section 4. Finally, some conclusions based on the results are drawn in section 5.

## 2. OVERVIEW OF RELATED WORKS IN DURBAN AND OTHER REGIONS

In Durban (29°52'S, 30° 58'E), South Africa, researchers have studied rainfall attenuation and drop size distribution and established the suitability of the lognormal and gamma models for DSD modeling in the region. *Odedina* and *Afullo* [11], proposed the lognormal and the modified gamma distribution models as best fit for the measurements of rainfall in Durban. *Afullo* [12], while studying the rain drop size distribution model for the eastern coast of South Africa established that the optimized lognormal and gamma DSD models compete favorably well with the DSD obtained for same tropical regions using the Biweight kernel estimation technique.

While using the maximum likelihood estimation (MLE) method, *Owolawi* [13], also proposed the lognormal model as best fit for DSD modeling in Durban. In their study, *Alonge* and *Afullo* [14], considered the DSD for different seasons- summer, autumn, winter and spring; they established that the lognormal model is suitable for summer and autumn; the modified gamma for winter and Weibull distribution is best for the spring season in Durban. The values of  $R_{0.01}$  for the different season were also estimated. *Akuon* and *Afullo* [15], derived the rain cell sizes the southern Africa and estimated the overall  $R_{0.01}$  for Durban as 60 mm/hr. The method of moments (MoM) and the maximum likelihood estimation (MLE) techniques were compared to estimate the parameters of the lognormal distribution model by *Adetan* and *Afullo* [16], using the DSD measurements in Durban for microwave propagation in South Africa. They concluded that the method of moment provides a better estimate of the DSD parameters in southern Africa with the lognormal model giving the best fit. *Adetan* and *Afullo* [17], showed that the three-parameter lognormal DSD gives a better fitting and performance when compared with the gamma distribution model. However, the gamma distribution model is also suitable as the error deviation is minimal at low rain rates.

Recently, *Adetan* and *Afullo* [18], analyzed the critical diameters for rainfall attenuation in southern Africa and concluded that the highest contribution of raindrops diameters to the specific rain attenuation was created by drop diameters not exceeding 2 mm, especially at higher frequencies in Durban. In their findings, the total percentage fraction created by raindrops in the diameter range  $0.5 \text{ mm} \leq D \leq 2.5 \text{ mm}$

and  $1 \text{ mm} \leq D \leq 3 \text{ mm}$  to the total specific attenuation is found to be critical for the overall and seasonal rainfall attenuation at 2.5 GHz-100 GHz in Durban. Similarly, within and outside the tropical region, a good number of researchers have also investigated the particular contributions of certain drop diameters to the specific rain attenuation. These include: *Fiser* [19], in the Czech Republic, *Lakshmi et al.* and *Lee et al.* [20,21], in Singapore, *Marzuki et al.* [22], in the Equatorial Indonesia and *Lam et al.* [23], in Malaysia. They concluded that small and medium-size drops contributed more to the rainfall attenuation as frequency increases.

## 3. DSD MEASUREMENTS, MODELS AND SPECIFIC ATTENUATION

### 3.1 Drop Size Distribution Measurements

The data used in this work is obtained from the Joss-Waldvogel (JW) RD-80 disdrometer mounted at the roof top of Electrical, Electronic and Computer Engineering building of the University of KwaZulu Natal South Africa. Although over 80000 data samples have been gathered between 2008 and 2010 since the installation of the instrument in September 2008, only the rain events of 27<sup>th</sup> December 2008 was used for the purpose of determining the contributions of specific channels to the overall rainfall rate and specific attenuation due to rain in Durban. The J-W RD-80 disdrometer converts the momentum of each of falling raindrop impacting on the sensor's surface into an electrical pulse of commensurate voltage [24]. The detectable diameter range is divided into 20 channels of varying diameters between 0.359-5.373 mm. The sampling area,  $A$  of the disdrometer is  $50 \text{ cm}^2$  ( $0.005 \text{ m}^2$ ) and sampling time,  $T$  is 60s. It is needful to mention that rainfall samples with overall sum of drops less than 10 were ignored from the data samples to compensate for the dead- time errors. The instrument is located at an altitude of 139.7m above sea level. The location site is shielded from abnormal winds and free of undue noise. The raindrop size distribution  $N(D)$  in  $\text{m}^{-3} \text{ mm}^{-1}$  is computed from the disdrometer measurements using (1) as given by [24, 25]:

$$N(D_i) = \frac{n_i}{v(D_i) * A * T * dD_i} \quad (1)$$

where  $n_i$  is the number of drops per channel,  $v(D_i)$  is the Gun-Kinzer [26] terminal velocity of water droplets and  $dD_i$  is the change in diameter of the channel in mm. Table 1 shows the threshold of the drop size channels and the measured drops for the selected rain rates. The asterisks (\*) in the table represent lack of rain drops in the channel. This lack of raindrops appears to be noticeable at lower channels as the rain rate increases. This will be discussed in more details in section 4.

The rainfall rate,  $R$  ( $mm/hr$ ) is calculated from the disdrometer data using (2) given by [25]:

$$R = \sum_{i=1}^{20} \frac{\pi}{6} D_i^3 n_i \frac{3600}{A.T} \quad (2)$$

A well-known integral equation of the rain rate  $R$  as computed from the DSD model is given by [26] with the associated discrete form as (3):

$$R = 6\pi \times 10^{-4} \int_0^{\infty} D_i^3 \cdot v(D_i) \cdot N(D_i) dD_i \quad (3)$$

$$= 1.88496 \times 10^{-3} \sum_{i=1}^{20} D_i^3 \cdot v(D_i) \cdot N(D_i) dD_i$$

Table 1: Drop size channels and measured drops from disdrometer measurements for the selected rain rates.

|                 |                           | Rain rate ( $mm/hr$ )/Time ( $min.$ ) |       |       |       |       |       |
|-----------------|---------------------------|---------------------------------------|-------|-------|-------|-------|-------|
|                 |                           | 20:53                                 | 20:57 | 21:01 | 21:10 | 21:05 | 21:07 |
| Channels<br>$i$ | Mean<br>Diameter<br>$D_i$ | 1.71                                  | 4.46  | 22.97 | 64.66 | 77.70 | 84.76 |
| 1               | 0.359                     | 1                                     | 11    | 20    | *     | *     | *     |
| 2               | 0.455                     | 4                                     | 10    | 47    | 1     | *     | *     |
| 3               | 0.551                     | *                                     | 10    | 45    | 1     | 5     | 4     |
| 4               | 0.656                     | 9                                     | 29    | 41    | 10    | 19    | 3     |
| 5               | 0.771                     | 9                                     | 47    | 41    | 14    | 19    | 15    |
| 6               | 0.913                     | 6                                     | 41    | 44    | 56    | 60    | 47    |
| 7               | 1.112                     | 16                                    | 40    | 75    | 124   | 123   | 143   |
| 8               | 1.331                     | 15                                    | 61    | 64    | 120   | 118   | 138   |
| 9               | 1.506                     | 5                                     | 36    | 44    | 114   | 98    | 116   |
| 10              | 1.656                     | 5                                     | 26    | 34    | 99    | 86    | 148   |
| 11              | 1.912                     | 10                                    | 20    | 108   | 171   | 168   | 225   |
| 12              | 2.259                     | 8                                     | 4     | 63    | 170   | 124   | 144   |
| 13              | 2.584                     | *                                     | 1     | 29    | 94    | 87    | 103   |
| 14              | 2.869                     | *                                     | *     | 16    | 61    | 60    | 49    |
| 15              | 3.198                     | *                                     | *     | 11    | 53    | 51    | 44    |
| 16              | 3.544                     | *                                     | *     | 4     | 10    | 34    | 34    |
| 17              | 3.916                     | *                                     | *     | 2     | 9     | 28    | 24    |
| 18              | 4.35                      | *                                     | *     | *     | *     | 9     | 10    |
| 19              | 4.859                     | *                                     | *     | *     | *     | *     | 4     |
| 20              | 5.373                     | *                                     | *     | *     | *     | *     | *     |
| Sum of drops    |                           | 88                                    | 336   | 688   | 1107  | 1089  | 1251  |

This computation is necessary in order to compare the measured rain rates and the observed contribution of individual channels on the overall rain rate and on the modeled  $N(D)$ .

### 3.2.1 Gamma DSD Model

The three parameter gamma DSD model is expressed by [8] as:

$$N(D) = N_0 D_i^\mu \exp(-\Lambda D_i) \quad [m^{-3} mm^{-1}] \quad (4)$$

where  $\mu$  is the shape parameter,  $N_0$  ( $m^{-3} mm^{-1-\mu}$ ) indicates the raindrop concentration of the DSD and  $\Lambda$  is the scale parameter in  $mm^{-1}$ . The distribution is

particularly useful in tropical regions where the exponential distribution has been found on numerous occasions to be inadequate (see, for example [8]). The shape parameter is assumed to be 2 while  $N_0$  and  $\Lambda$  are estimated as [17]:

$$\left. \begin{aligned} N_0 &= 78259 R^{-0.156} \\ \Lambda &= 6.3209 R^{-0.168} \\ \mu &= 2 \end{aligned} \right\} \quad (5)$$

### 3.2.2 Lognormal DSD Model

The lognormal distribution model was proposed by [9,10] was primarily for modeling DSD in the tropical region and expressed in the form of (6) as:

$$N(D) = \frac{N_T}{\sigma D \sqrt{2\pi}} \exp \left[ -0.5 \frac{(\ln(D) - \mu)^2}{\sigma^2} \right] \quad (6)$$

where  $\mu$  is the mean of  $\ln(D)$ ,  $\sigma$  is the standard deviation which determines the width of the distribution and  $N_T$  depends on climates, geographical location of measurements and rain types. The lognormal distribution model is more advantageous in the sense that each of its parameters have a clear physical significance. Moreover, the parameters ( $N_T$ ,  $\mu$  and  $\sigma^2$ ) are linearly related to the moments of drop size distribution. Therefore, it is considered adequate for describing the DSD in this region [27]. The three parameters in (6) are related to  $R$  as:

$$\left. \begin{aligned} N_T &= a_0 R^{b_0} \\ \mu &= A_\mu + B_\mu \ln R \\ \sigma^2 &= A_\sigma + B_\mu \ln R \end{aligned} \right\} \quad (7)$$

where  $a_0, b_0, A_\mu, B_\mu, A_\sigma$  and  $B_\sigma$  are coefficients of moment regression determined using the least squares method of regression technique. These parameters have been estimated for Durban using the method of moments in [17] and represented in (8) as:

$$\left. \begin{aligned} N_T &= 268.07 R^{0.4068} \\ \mu &= -0.3104 + 0.1331 \ln R \\ \sigma^2 &= 0.0738 + 0.0099 \ln R \end{aligned} \right\} \quad (8)$$

### 3.3 Specific Rain Attenuation

The estimation or prediction of rainfall attenuation in both satellite and terrestrial communication applications is very necessary. The specific rain attenuation  $\gamma$  ( $dB/km$ ) due to rain,  $R$  ( $mm/hr.$ ) is given by [28] as (9):

$$\gamma = 4.343 \times 10^{-3} \int_0^{\infty} Q_t(D) \cdot N(D) dD \quad (9)$$

where  $Q_t(D)$  is the extinction cross section which depends on the raindrop diameter  $D$ , the wavelength  $\lambda$ , and the complex refractive index of water drop  $m$ ,  $N(D)dD$  is the number of raindrops per unit volume where the diameter of the equivalent volume spherical drop is between  $D$  and  $D+dD$ . The extinction cross section  $Q_t(D)$  can further be expressed by [29, 30] as:

$$Q_t(D) = \frac{\lambda^2}{2\pi} \sum_{n=1}^{\infty} (2n+1) \text{Re}[a_n + b_n] \quad (10)$$

where  $a_n$  and  $b_n$  are the Mie scattering coefficients. The extinction cross section is calculated by applying the classical scattering theory of Mie for a plane wave impinging upon a spherical absorbing particle. The Mie scattering theory is applied under the assumption that each spherical raindrop illuminated by a plane wave is uniformly distributed in a rain filled medium. Similarly, it is assumed that the distance between each drop is large enough to avoid any interaction between them. The extinction cross section,  $Q_t(D)$  provided by [11] as a frequency-dependent, power law function with coefficients  $\kappa$  and  $\alpha$  is given in (11) and adopted in this work. It should be mentioned that the absorption and scattering can be modelled by different methods depending on the frequency of the signal and the shape of the raindrop. Examples of such methods include the use of Rayleigh theory, Mie theory and the T-matrix technique. The Rayleigh approximation applies to frequencies lower than the frequency considered in this work. The Mie theory assumes that the shape of the raindrop is spherical, which is not the case for raindrops above 2 mm in diameter. The T-matrix can model axisymmetric particles, which improves the representation of a raindrop and hence increases the accuracy of attenuation estimates.

$$Q_t(D) = \kappa \left(\frac{D}{2}\right)^{\alpha} \quad (11)$$

where  $\kappa$  and  $\alpha$  are the coefficients that depend on a number of parameters such as temperature, raindrop size distribution, raindrop shape, frequency of transmission and polarization to a certainty [31]. The Mätzler's MATLAB [32] functions are used to compute  $\kappa$  and  $\alpha$  values at  $f = 19.5 \text{ GHz}$ . The computed values of  $\kappa$  and  $\alpha$  at  $f = 19.5 \text{ GHz}$  are 1.6169 and 4.2104 respectively with the complex refractive index of water drop,  $m = 6.7332 + j2.7509$  of the scattering amplitudes.

However, Olsen *et al.* [33] further approximated (9) in a power law as a function of rain rate  $R$ , given as:

$$\gamma = \kappa R^{\alpha} \quad (12)$$

In this work, we analyze the specific contribution of individual raindrop channels to the overall measured rainfall rate and specific rainfall attenuation in southern Africa. The Mie scattering functions at  $20^\circ\text{C}$  is employed to calculate the scattering functions at frequency  $f = 19.5 \text{ GHz}$  with the assumption that the raindrops are spherical in shape. Each particle is assumed to be a homogeneous sphere and the incident field is assumed to be a plane wave. The three parameter lognormal and gamma DSD models as determined in [17] for Durban are used to characterize the measured drop size distribution  $N(D)$ . The three-parameter model ensures high representability of the experimented measurements.

## 4. RESULTS AND ANALYSIS

### 4.1 Rain rate, drop size distributions $N(D)$ and raindrop diameters

The drops size distribution is an essential parameter for the evaluation of the rainfall attenuation at microwave and millimeter wave frequencies. Fig. 1 shows the measured drop size distribution,  $N(D)$  from the disdrometer data using (1) and the drop diameters for the selected rain rates. The drop diameter increases as the rain rates increases. Fig. 2 shows the modeled and measured  $N(D)$  with respect to the drop diameters for the gamma and lognormal DSD models using the parameters in (5) and (8) and rain rate of  $84.76 \text{ mm/hr}$ . Although, the two models overestimate the measured DSD at the lower and larger diameters, the gamma model overestimates more at lower diameters than the lognormal model. This may be due to the parameter estimation.

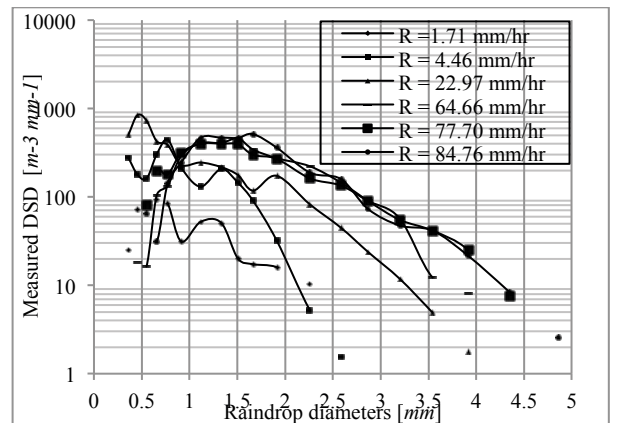


Figure 1: Measured raindrop size distributions for the selected rain rate values [using (1)].

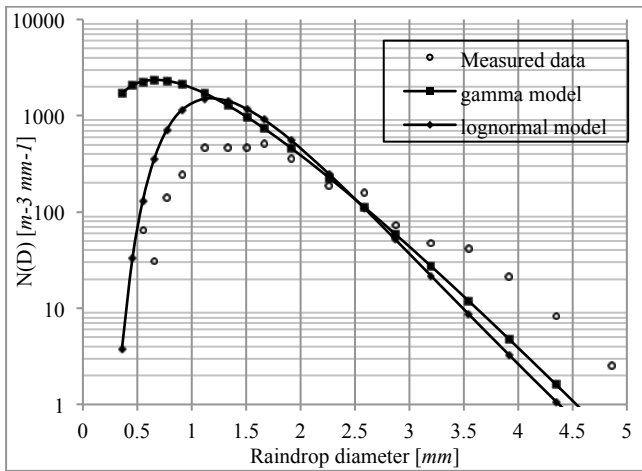
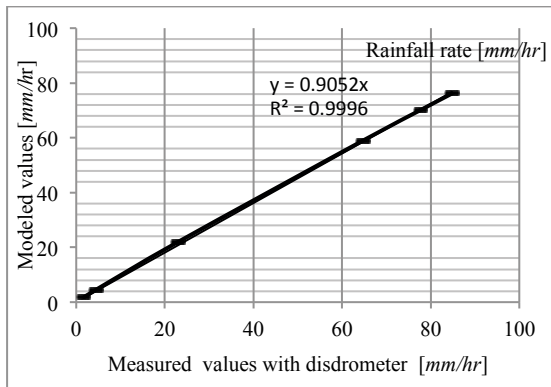
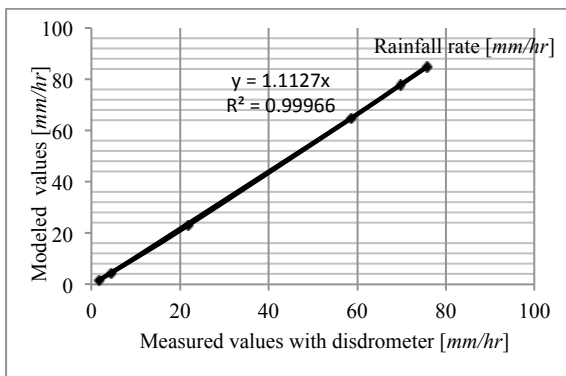


Figure 2: Comparison of the measured and modeled  $N(D)$  with drop diameters.

In Fig. 3, a comparison of the modeled values of the rain rates with the actual disdrometer measured values is shown for gamma and lognormal models. A good agreement is observed between the measured and estimated values of the rain rates.



(a)



(b)

Figure 3: Comparison between measured and modeled rain rate values for (a) gamma and (b) lognormal models.

#### 4.2 Estimation of the specific rainfall attenuation and raindrop channels

The specific rainfall attenuation is calculated using (4, 6, 9, and 11). The computed values of  $\kappa$  and  $\alpha$  are used. There is an agreement between the two models with respect to rain rate as shown in Fig. 4. The contributions of individual channels and removal of consecutive channels to the specific rain attenuation is illustrated in Tables 2 to 4 for the two models at  $f = 19.5 \text{ GHz}$ . It can be observed that the roles of smaller raindrop diameters to the specific attenuation are insignificant (negligible). Their removals produce least attenuation when compared to the larger diameters (Tables 3 and 4).

#### 4.3 Contributions of raindrop channels to overall rain rates

The range of raindrop channels is studied by removing the individual channels and the effect on the measured rain rate observed. Fig. 5 shows the difference between the measured rain rates with the individual channels containing raindrops removed. Firstly, the individual channel with raindrops is removed consecutively and the effect on the overall rain rate is observed. That is, channel 1 is removed, and then channels 1 and 2, channels 1 to 3 and so on. Thereafter, the channels are removed (with or without raindrops) in an alternate manner such that channel 1 is removed first, then channels 1 and 20, channels 1,2 and 20, then channels 1,2, 19 and 20 and so on and the effect on the overall rain rate is observed.

In general and for the two models considered, the removal of smaller diameters (channels 1 to 5) does not alter significantly the total rain rates. As the number of channels removed increases, the deviation tends to increase sharply as observed from Fig.4 for all the rain rates. The critical raindrop channels lies at the center of the disdrometer channel for  $D \geq 0.771 \text{ mm}$ . Similarly, as observed from Table 1, the largest raindrops for the lower rain rate are observed in channels 7 and 8 and as the rain rate increases, there seems to be no raindrops in the first 2 channels. At high rain rates, the largest (maximum) raindrops occur in channel 11 (1.912mm). This further confirms that the roles of the channels in the diameter range  $D \geq 0.771 \text{ mm}$  are critical in the overall rain rate. Hence, raindrops size distribution and the drop diameters (channels) are significant to the overall rain rate estimation.

4.4 Root Mean Square Error (RMSE)

The root mean square (RMS) error used for assessing the deviation of the estimated rain rate from the measured is given as (13):

$$RMS_{deviation} = \sqrt{\frac{1}{n} \sum_{i=1}^n [\hat{F}(X_i) - F(X_i)]^2} \quad (13)$$

confirms the suitability of these models for DSD modeling in Durban.

where  $\hat{F}(X_i)$  is the estimated rain rate values obtained from the model using (3),  $F(X_i)$  is the measured rain rate using (2) and  $n$  is the number of channels containing raindrops. It was observed that the values of root mean square deviation (RMS) error using the two models are low even at high rain rates. This is shown in Table 5. They are slightly different from each other and this further

Table 2: Specific rain attenuation (dB/km) with channels (containing raindrops) removed at  $f=19.5GHz$ .

| R<br>(mm/hr) | Gamma Model(G-M)         |      |      |      |      |      | Lognormal Model (Ln-M)   |                 |      |      |      |      |  |  |
|--------------|--------------------------|------|------|------|------|------|--------------------------|-----------------|------|------|------|------|--|--|
|              | Channel removed          |      |      |      |      |      |                          | Channel removed |      |      |      |      |  |  |
|              | With no channels removed | 1    | 2    | 3    | 4    | 5    | With no channels Removed | 1               | 2    | 3    | 4    | 5    |  |  |
| 1.71         | 0.09                     | 0.09 | 0.09 | 0.09 | 0.08 | 0.08 | 0.09                     | 0.09            | 0.09 | *    | 0.08 | 0.08 |  |  |
| 4.46         | 0.26                     | 0.26 | 0.26 | 0.26 | 0.25 | 0.25 | 0.26                     | 0.26            | 0.26 | 0.26 | 0.25 | 0.24 |  |  |
| 22.97        | 1.46                     | 1.46 | 1.46 | 1.46 | 1.45 | 1.44 | 1.44                     | 1.44            | 1.44 | 1.44 | 1.44 | 1.43 |  |  |
| 64.66        | 4.35                     | *    | 4.35 | 4.35 | 4.34 | 4.32 | 4.29                     | *               | 4.29 | 4.29 | 4.29 | 4.28 |  |  |
| 77.70        | 5.28                     | *    | *    | 5.27 | 5.26 | 5.25 | 5.21                     | *               | *    | 5.21 | 5.21 | 5.20 |  |  |
| 84.76        | 5.78                     | *    | *    | 5.78 | 5.77 | 5.75 | 5.71                     | *               | *    | 5.71 | 5.71 | 5.70 |  |  |

Table 3: Specification rain attenuation (dB/km) with consecutive channels removed starting with lower channels at  $f=19.5 GHz$ .

| R<br>(mm/hr) | Gamma Model(G-M)         |      |      |      |      |      | Lognormal Model (Ln-M)   |                  |      |      |      |      |  |  |
|--------------|--------------------------|------|------|------|------|------|--------------------------|------------------|------|------|------|------|--|--|
|              | Channels removed         |      |      |      |      |      |                          | Channels removed |      |      |      |      |  |  |
|              | With no channels removed | 1    | 1-2  | 1-3  | 1-4  | 1-5  | With no channels removed | 1                | 1-2  | 1-3  | 1-4  | 1-5  |  |  |
| 1.71         | 0.09                     | 0.09 | 0.09 | 0.89 | 0.08 | 0.07 | 0.09                     | 0.09             | 0.09 | 0.09 | 0.08 | 0.07 |  |  |
| 4.46         | 0.26                     | 0.26 | 0.26 | 0.25 | 0.24 | 0.23 | 0.26                     | 0.26             | 0.26 | 0.25 | 0.25 | 0.24 |  |  |
| 22.97        | 1.46                     | 1.46 | 1.46 | 1.45 | 1.44 | 1.42 | 1.44                     | 1.44             | 1.44 | 1.44 | 1.44 | 1.43 |  |  |
| 64.66        | 4.35                     | 4.35 | 4.35 | 4.34 | 4.33 | 4.30 | 4.29                     | 4.29             | 4.29 | 4.29 | 4.29 | 4.28 |  |  |
| 77.70        | 5.28                     | 5.28 | 5.28 | 5.27 | 5.25 | 5.22 | 5.21                     | 5.21             | 5.21 | 5.21 | 5.21 | 5.20 |  |  |
| 84.76        | 5.78                     | 5.78 | 5.78 | 5.77 | 5.76 | 5.72 | 5.71                     | 5.71             | 5.71 | 5.71 | 5.70 | 5.69 |  |  |

Table 4: Specific rain attenuation (dB/km) with consecutive channels removed starting with larger channels using the lognormal model at  $f=19.5GHz$

| R<br>(mm/hr) | Channels removed         |      |       |       |       |       |
|--------------|--------------------------|------|-------|-------|-------|-------|
|              | With no channels removed | 20   | 19-20 | 18-20 | 17-20 | 16-20 |
| 1.71         | 0.09                     | 0.09 | 0.09  | 0.09  | 0.08  | 0.09  |
| 4.46         | 0.26                     | 0.26 | 0.26  | 0.26  | 0.26  | 0.26  |
| 22.97        | 1.44                     | 1.44 | 1.44  | 1.43  | 1.43  | 1.42  |
| 64.66        | 4.29                     | 4.29 | 4.26  | 4.22  | 4.12  | 3.99  |
| 77.70        | 5.21                     | 5.20 | 5.16  | 5.09  | 4.95  | 4.76  |
| 84.76        | 5.71                     | 5.69 | 5.65  | 5.56  | 5.39  | 5.17  |

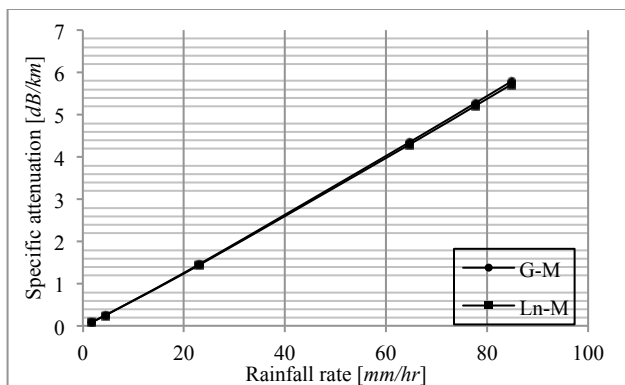
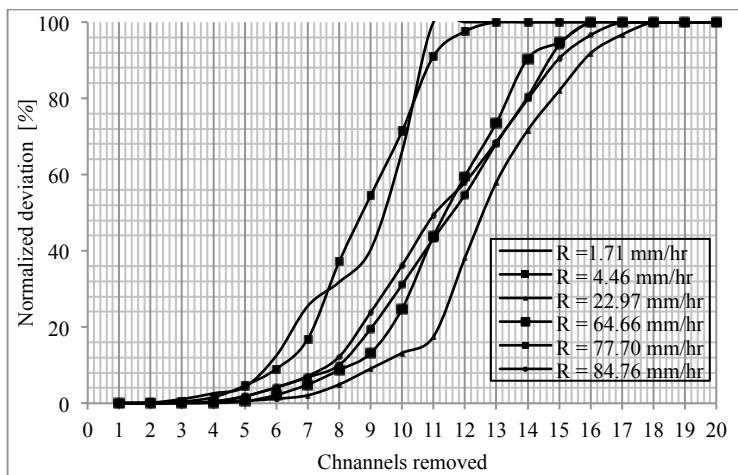
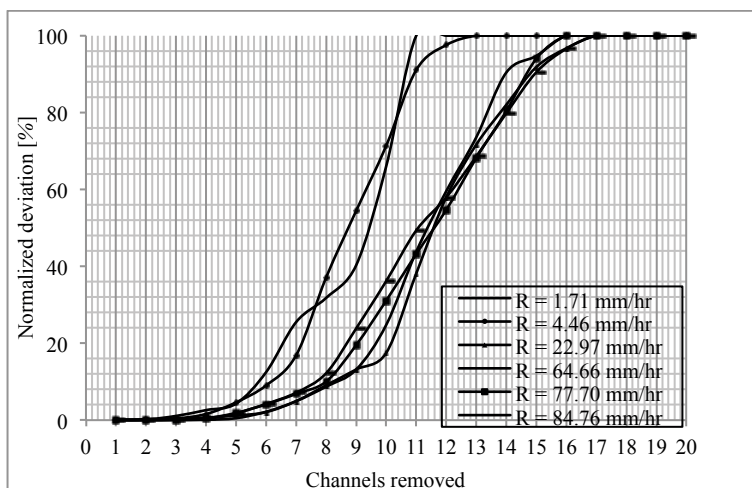


Figure 4: Specific rain attenuation at  $f=19.5\text{GHz}$  for the models.



(a)



(b)

Figure 5: Normalized deviation for channels removal (a) Gamma (b) lognormal models

Table 5: Estimation of root mean square deviation between measured and modeled rain rate.

| $R$ (mm/hr.) | Gamma | Lognormal |
|--------------|-------|-----------|
| 1.71         | 0.01  | 0.02      |
| 4.46         | 0.01  | 0.02      |
| 22.97        | 0.29  | 0.24      |
| 64.66        | 1.53  | 1.42      |
| 77.70        | 2.00  | 1.88      |
| 84.76        | 2.21  | 2.08      |

## 5. CONCLUSION

The paper presents the contribution of individual raindrop channels to the overall rain rate and specific rainfall attenuation in southern Africa. The six measured rain rate values recorded per minute using the J-W RD-80 disdrometer was used in analysis. These rain rate values also represent the stratiform and convective types of rainfall. Smaller channels were found to contribute little to the overall measured rain rates and produce least rain attenuation with the removal of the bins. The amount of attenuation produced with the removal of the larger diameters is significant. A comparative analysis of the error deviation shows that the lognormal DSD model gives a better performance as the rain rate increases from stratiform to convective. The removal of lower channels does not alter the attenuation and can be ignored while estimating the specific rain attenuation. However, larger diameters produce significant effect on the specific rain attenuation especially at very high rain rates. We conclude therefore that the smaller channels (1-4) can be ignored while estimating the rain rate and specific attenuation as they do not alter significantly the estimated values. The major contribution to the overall measured rain rate is formed by diameter  $D \geq 0.771\text{mm}$ . These critical diameters and attenuation statistics are essential to properly design adequate fade margin levels and for the purpose of link budget design by service providers and system engineers in the region.

## 6. REFERENCES

- [1] C. Capsoni, L. Luini, A. Paraboni, C. Riva and A. Martelluci: "A new prediction model of rain attenuation that separately accounts for stratiform and convective rain," *IEEE Trans. on Antennas and Propagation*, vol. 57, no.1, pp.196-204, January 2009.
- [2] M. Cheffena: "Measurement analysis of amplitude scintillation for terrestrial line-of-sight links at 42 GHz," *IEEE Trans. on Antennas and Propagation*, vol. 58, no.6, pp. 2021-2028, June 2010.
- [3] J. M. Garcia-Rubia, J.M. Riera and P. Garcia-del-Pino: "Propagation in the Ka band: Experimental characterization for satellite applications," *IEEE Antennas and Propagation Magazine*, vol. 53, no.2, pp. 65-76, April 2011.
- [4] G. Hendratoro and I. Zawadzki: "Derivation of parameters of Y-Z power-law relation from raindrop size distribution measurements and its application in the calculation of rain attenuation from radar reflectivity factor measurements," *IEEE Trans on antenna and propagation*, vol. 51, no. 1, 2003
- [5] A. Safaai-Jazi, H. Ajaz and W.L. Stutzman: "Empirical models for rain fade time on Ku- and Ka- band satellite links," *IEEE Trans. on Antennas and Propagation*, vol. 43, no.12, pp.1411-1415, December 1995.
- [6] J.S. Marshall and W.M. Palmer: "The distribution of raindrops with size," *J. Meteor.* 5, pp.165-166, 1948.
- [7] J.O. Laws and D.A. Parsons: "The relation of raindrops size to intensity," *Trans. Atm. Geophys. Union*, 24, pp. 452-460, 1943.
- [8] D. Atlas and C.W. Ulbrich: "The Physical basis for attenuation-rainfall relationships and the measurement of rainfall parameters by combined attenuation and radar methods," *J. Rech. Atmos.*, 8, pp.275-298, 1974.
- [9] G.O. Ajayi and R.L. Olsen: "Modeling of a tropical raindrop size distribution for microwave and millimeter wave applications," *Radio Sci.* vol. 20, no 2, pp.193-202, 1985.
- [10] I.A. Adimula and G.O. Ajayi: "Variations in raindrop size distribution and specific attenuation due to rain in Nigeria," *Annals of Telecommunications*, 51, no. 1-2, 1996.
- [11] M.O. Odedina and T.J. Afullo: "Determination of rain attenuation from electromagnetic scattering by spherical raindrops: Theory and experiment," *Radio Sci.* vol. 45, 2010.
- [12] T.J.O. Afullo: "Raindrop size distribution modeling for radio link along the Eastern coast of South Africa," *PIERS B*, vol.34, pp.345-366, 2011.



- [13] P. Owolawi: "Raindrop size distribution model for the prediction of rain attenuation in Durban," *PIERS ONLINE*, vol.7, no.6, pp.516-523, 2011.
- [14] A.A. Alonge and T.J. Afullo: "Seasonal analysis and prediction of rainfall effects in Eastern South Africa at microwave frequencies," *PIERS B*, vol.40, pp. 279-303, 2012.
- [15] P.O. Akuon and T.J. Afullo: "Rain cell sizing for the design of high capacity radio link system in South Africa," *PIERS B*, vol. 35, pp. 263-285, 2011.
- [16] O. Adetan and T.J. Afullo: "Comparison of two methods to evaluate the lognormal raindrop size distribution model in Durban," *The Southern Africa Telecommunication Networks and Applications Conference (SATNAC)*, Fancourt, Western Cape, South Africa, 2012.
- [17] O. Adetan and T.J. Afullo: "Three-parameter raindrop size distribution modeling for microwave propagation in South Africa," *Proceedings of The International Association of Science and Technology for Development (IASTED)*, International Conference on Modeling and Simulation (Africa MS 2012) Gaborone, Botswana, DOI:10-2316/P.2012.761-027, pp. 155-160, 2012.
- [18] O. Adetan and T.J. Afullo: "The critical diameters for rainfall attenuation in Southern Africa," *PIERS B*, vol. 46, pp.275-297, 2013.
- [19] O. Fiser: "The role of particular rain drop size classes on specific rain attenuation at various frequencies with Czech data example," *Proceedings of ERAD*, pp. 113-117, 2002.
- [20] S. Lakshmi, Y.H. Lee and J.T. Ong: "The roles of particular raindrop size on rain attenuation at 11GHz," *IEEE Xplore*, 1-4244-0983-7/07, ICICS, 2007.
- [21] Y.H. Lee, S. Lakshmi and J.T. Ong: "Rain drop size distribution modeling in Singapore-critical diameters," *The Second European Conference on Antennas and Propagation (EUCAP)*, November11-16, 2007.
- [22] M. Marzuki, T. Kozu, T. Shimomai, W.L. Randeu, H. Hashiguchi and Y. Shibagaski: "Diurnal variation of rain attenuation obtained from measurement of raindrop size distribution in Equatorial Indonesia," *IEEE Trans. on Antennas and Propagation*, vol.57, no.4, pp.1191-1196, April 2009.
- [23] H.Y. Lam, J. Din, L. Luini, A.D. Panagopoulos, and C. Capsoni: "Analysis of raindrop size distribution characteristics in Malaysia for rain attenuation prediction," *IEEE Xplore General Assembly and Scientific Symposium, XXXth URSI*, August 13-20, 2011
- [24] J. Joss, J.C. Thams and A. Waldvogel: The variation of raindrop-size distribution at Locarno," *Proceedings of International Conference on Cloud Physics*, pp. 369-373, 1968
- [25] M.J. Bartholomew: "Disdrometer and tipping bucket rain gauge handbook," *ARM Climate Research Facility*, DOE/SC-ARM/TR-079, December 2009.
- [26] R. Gunn and G.D. Kinzer: "Terminal velocity of fall for water drops in stagnant air," *J. Appl. Meteorology*, 6, pp.243-248, 1949.
- [27] K.I. Timothy, J.T. Ong and E.B.L. Choo: "Raindrop size distribution using method of moments for terrestrial and satellite communication applications in Singapore," *IEEE Trans. on Antennas and Propagation*, vol. 50, no.10, pp.1420-1424, October 2002.
- [28] G.O. Ajayi, S. Feng, and S.M. Radicella, B.M. Reddy (Ed): Handbook on radio propagation related to satellite communications in tropical and subtropical countries. ICTP, Trieste, Italy, pp.7-14, 1996.
- [29] H.C. Van de Hulst: "Light Scattering by Small Particles," John Wiley and Sons Inc., New York, 1957.
- [30] C.F. Bohren and D.R. Huffman: "Absorption and Scattering of Light by Small Particles," John Wiley, Wienheim, 2004.
- [31] Z.X. Zhou, L.W. Li, T.S. yeo and M.S. Leong: "Cumulative distributions of rainfall rate and microwave attenuation in Singapore's tropical region," *Radio Sci.*, vol. 35, no.3, pp. 751-756, 2000.
- [32] C. Mätzler: "Drop-size distributions and Mie computation," IAP Research Report 2002-16, University of Bern, Bern, November 2002
- [33] R.L. Olsen, D.V. Rogers and D.B Hodge: The  $aR^b$  relation in the calculation of rain attenuation," *IEEE Trans. on Antennas and Propagation*, 26(2), pp.547-556, 1978

#### APPENDIX

The normalized deviation of Figs. 5 (in %) as used in [27] is adopted in this work. It is calculated using the true measured rain rate and the rain rate with some of the bins (channels) removed. The equation is given as:

$$N(D_j)[\%] = \frac{[R_{(true)} - R_{(jth\ bin\ removed)}]}{R_{(true)}} \times 100 \quad (1)$$

where  $R_{(true)}$  is obtained from (2) and  $R_{(jth\ bin\ removed)}$  is also obtained from (2) but with some of the bins removed.

